RSC Advances

PAPER

View Article Online
View Journal | View Issue

Cite this: *RSC Adv.*, 2017, **7**, 48058

A fluorescence switching sensor based on graphene quantum dots decorated with Hg^{2+} and hydrolyzed thioacetamide for highly Ag^{+}-sensitive and selective detection

Pimpisa Kaewanan,[a] Phitchan Sricharoen,[a] Nunticha Limchoowong,[a] Thitiya Sripakdee,[b] Prawit Nuengmatcha[c] and Saksit Chanthai *[a]

A selective fluorescent sensor based on graphene quantum dots (GQDs) was developed for the determination of silver ions (Ag^{+}). The GQDs were prepared by the citric acid pyrolysis method. In the presence of mercury ions (Hg^{2+}), the fluorescence intensity of the GQDs decreased linearly and it was fully recovered by the hydrolysis of thioacetamide (TAA), giving hydrogen sulfide in the reaction system. This research study was aimed at using the fluorescence turn-off sensor for the selective determination of Ag^{+}. Upon the addition of Ag^{+}, the fluorescence intensity of the generated sulfide-(Hg^{2+} quenched GQDs) decreased as a linear function of the Ag^{+} concentration. Then, the acquired GQDs showed steady, selective, and highly sensitive detection of Ag^{+}. The experimental parameters affecting the fluorescence turn-on/off sensor were investigated and optimized. The optimum conditions included 4 μM Hg^{2+} concentration, 70 μM TAA concentration, solution pH of 7 and a 5 min reaction time. Under the optimized conditions, the working linear concentration range, limit of detection and limit of quantification for Ag^{+} were 0.5–10.0, 0.18 and 0.60 μM, respectively. The proposed method was successfully applied for the selective determination of trace amounts of Ag^{+} in five real water samples with satisfying levels of recovery (89.31–114.08%).

Received 17th August 2017
Accepted 2nd October 2017

DOI: 10.1039/c7ra09126e

rsc.li/rsc-advances

Introduction

Silver ions (Ag^{+}) are included in the list of heavy metal ions, and their potential toxicity for the environment and human body has drawn people's attention. Owing to their broad employment in many industries, such as electronics, photography, mirrors, and pharmacy, a large amount of silver is released into the environment annually from industrial waste and emissions, especially into sludge waste and even surface waters.[1,2] It has also been found that silver is toxic to humans at concentrations as high as 0.9 μM in drinking water.[3] Considering these facts, applying a simple, rapid and accurate method to monitor silver ions at trace levels in various samples is of great importance. Various techniques have been used for the determination of silver in real samples, such as the spectrophotometric method,[4] graphite furnace atomic absorption spectroscopy (GFAAS),[5] high-resolution continuum source flame atomic absorption spectrometry (HR-CS FAAS),[6] inductively coupled plasma optical emission spectrometry (ICP-OES),[7] differential pulse anodic stripping voltammetry (DPASV),[8] and spectrofluorimetry.[9,10] Although these techniques are highly sensitive and selective, they require tedious sample preparation and preconcentration procedures, expensive instruments, and professional personnel.

Recently, nanomaterials have been used to build sensitive analytical sensors for the analysis of various inorganic and organic substances including trace amounts of hazardous substances in the environment. Such sensors possess certain advantages, *e.g.* high sensitivity, short analysis time, low cost, and simple preparation and treatment.[11] Graphene quantum dots (GQDs) have generated enormous excitement because of their superiority in a variety of advantageous properties. They were discovered very recently as a class of zero-dimensional graphitic nanomaterials with lateral dimensions less than 100 nm, and they have either a single layer, double layers, or a few layers (3 to <10).[12,13] Compared with organic dyes and semiconductive quantum dots (QDs), GQDs are superior in terms of their excellent properties, such as their high photostability against photobleaching and blinking, biocompatibility and low toxicity.[15] Moreover, similar to graphene, GQDs have

[a]*Materials Chemistry Research Center, Department of Chemistry, Center of Excellence for Innovation in Chemistry, Faculty of Science, Khon Kaen University, 123 Mittraphab Road, Khon Kaen 40002, Thailand. E-mail: sakcha2@kku.ac.th; Fax: +66 43202373; Tel: +66 43009700 ext. 42174-5*

[b]*Chemistry Program, Faculty of Science and Technology, Sakon Nakhon Rajabhat University, Sakon Nakhon 47000, Thailand*

[c]*Department of Chemistry, Faculty of Science and Technology, Nakhon Si Thammarat Rajabhat University, Nakhon Si Thammarat 80280, Thailand*

excellent characteristics such as large surface areas, large diameters, fine surface grafting *via* the π–π conjugated network or surface groups, and other special physical properties.[16,17] Furthermore, the carboxyl and hydroxyl groups at their edge enable them to display excellent water solubility and suitability for successive functionalization with various organic, inorganic, polymeric or biological species. For these reasons, GQDs have attracted significant attention worldwide. From the literature, a small number of fluorescent sensors for Ag^+ have been reported compared with other metal sensors.[18–21] Furthermore, most of the fluorescent sensors for Ag^+ showed limitations in their practical application due to their low water solubility, serious toxicity even at relatively low concentrations, and other drawbacks. Hence, it remains essential to develop much simpler, more efficient and robust methods for silver ion probing that can be used for the selective detection of Ag^+ in real samples.

In this research, a selective fluorescent sensor for the determination of silver ions (Ag^+) was developed based on GQDs. The GQDs were prepared by the citric acid pyrolysis method. In the presence of mercury ions (Hg^{2+}), the fluorescence intensity of the GQDs decreased linearly and it was fully recovered by the hydrolysis of thioacetamide (TAA). This study is aimed at using a fluorescent sensor for the determination of Ag^+. Upon the addition of Ag^+, the fluorescence intensity of the TAA-(Hg^{2+} quenched GQDs) decreased as a linear function of the Ag^+ concentration. In addition, the optimum conditions including the Hg^{2+} and TAA concentrations, pH of the solution and reaction time were investigated in detail.

Experimental

Chemicals and reagents

All of the chemicals used were of analytical grade. The citric acid, sodium hydroxide, silver chloride, potassium chloride, and barium chloride were purchased from Ajax Fine Chem Pty. Ltd. (Australia). The mercury nitrate, cobalt nitrate hexahydrate, lead nitrate, zinc nitrate hexahydrate, cadmium nitrate tetrahydrate, copper nitrate trihydrate, potassium cyanide, potassium iodide, thioacetamide (99.0%), and sodium sulfide were purchased from Sigma-Aldrich (Germany).

Apparatus

UV-Vis absorption spectra were obtained using an Agilent 8453 spectrophotometer (Agilent, Germany). Emission spectra were recorded using an RF-5301PC spectrofluorophotometer (Shimadzu, Japan) with excitation and emission slit widths of 5 nm. A quartz cuvette (1 cm path length) was used for both the UV-visible absorption and fluorescence measurements. Transmission electron microscopy (TEM) images were obtained using a JEOL1200 (JEOL Ltd., Japan). The functional groups of the GQDs were characterized by an attenuated total reflectance-Fourier transform infrared (ATR-FTIR) spectrometer (TENSOR 27, Bruker, Germany). A pH meter (UB-10 Ultra Basic, Denver, USA) and analytical balance (AC121S, Sartorius, USA) were also used in this study.

Synthesis and characterization of the GQDs

The GQDs were prepared from citric acid by a pyrolysis method with a modified procedure.[12–14] Briefly, 2.0 g of citric acid was added into a 250 mL beaker. The beaker was heated to 200 °C using a paraffin oil bath for about 5 min. The solid citric acid was slowly liquated and had a yellow color. 100 mL of 0.25 M NaOH was added into the beaker with continuous stirring for 30 min at room temperature. The obtained sample solution was neutralized to pH 7 with HCl, and the GQD stock solution was stored at 4 °C before use.

The quenching effect of the GQDs using Hg^{2+}

20 μL of a 2.0 mg mL^{-1} GQD solution and 1 mL of 1 M phosphate buffer with a pH of 7.4 were mixed in a 10 mL volumetric flask. Then, various concentrations of Hg^{2+} were added to an aliquot of the GQD solution (10 mL final volume) at room temperature. The Hg^{2+} quenched fluorescence spectra of each of the GQD solutions were recorded immediately at $\lambda_{ex}/\lambda_{em}$ 370/460 nm. Then, such spectral measurements were used to plot the quenching calibration curve for Hg^{2+}.

To confirm the selectivity of the Hg^{2+} quenched GQDs, the following procedure was carried out. An individual stock solution of various metal ions (0.01 mM) was prepared by the dissolution of metal salts in ultrapure water. 10 μL of the GQD solution was mixed with 100 μL of 0.01 mM solutions of each of the metal ions (10 μM final concentration) and adjusted to a final volume of 10 mL in a volumetric flask with DI water.

The selectivity of the Hg^{2+}–GQDs fluorescence turn-on by the hydrolysis of TAA

The fluorescence measurement of the GQDs was performed using a 10 mL volumetric flask containing 20 μL of GQDs (2.0 mg mL^{-1}) mixed with 4 μM Hg^{2+} in a 0.1 M phosphate buffer solution with a pH of 7. Various concentrations of TAA and Na_2S as a reference were added to the solution mixture and adjusted to 10 mL with DI water. The emission spectra of the test solution were recorded with an excitation wavelength of 370 nm. In addition, the effect of the concentration of ammonium acetate solution was investigated in order to find out any common ion effects, *i.e.* acetate and ammonium ions, except hydrogen sulfide, generated by the hydrolysis of TAA.

The selectivity of the Hg^{2+}–GQDs–TAA fluorescence turn-off sensor for Ag^+ detection

The fluorescence measurement of the GQDs was performed using 20 μL of GQDs (2.0 mg mL^{-1}) mixed with 4 μM Hg^{2+} and 70 μM TAA in a 0.1 M phosphate buffer solution with a pH of 7. Various concentrations of Ag^+ were added to the mixture solution and adjusted to various pH values with a 10 mL final volume with DI water. The emission spectra of the test solution were also recorded with an excitation wavelength of 370 nm. Spectral measurements were used to plot the quenching calibration curve for Ag^+.

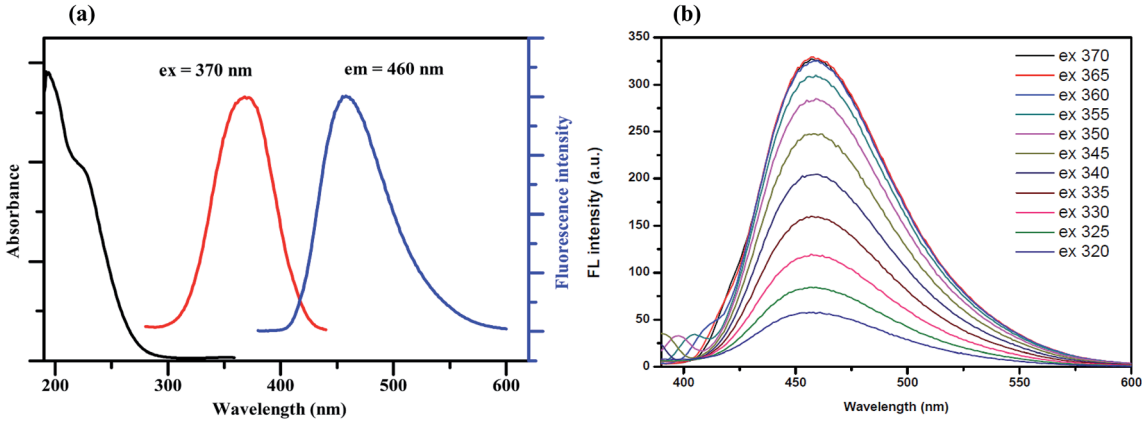

Fig. 1 (a) The absorption (black line), fluorescence excitation (red line) and fluorescence emission (blue line) spectra of the GQDs and (b) the fluorescence spectra of the GQDs at different excitation wavelengths.

The optimization of the conditions for the fluorescence turn-off sensor for Ag^{+}

The fluorescence measurement of the GQDs was performed in a phosphate buffer solution at a pH of 7 in a 10 mL volumetric flask. Briefly, 1 mL of the GQDs (200 mg L^{-1}) was mixed with 4 μM Hg^{2+} and 70 μM TAA in a 0.1 M phosphate buffer solution at a pH of 7. Then, various concentrations of Ag^{+} were added to the sample solution. Finally, the volume of the solution was adjusted to 10 mL with DI water. The emission spectra of the sample mixtures were recorded with a spectrofluorometer.

To obtain the optimum conditions of the proposed sensor, the following parameters were studied using the same procedure as mentioned above. The effect of the pH of the solution was studied by varying the pH of the solution from 3–12 using an acetate buffer (pH 3–5) and phosphate buffer (pH 6–12). The incubation times were studied from 0–1 h. The effect of the concentration of Hg^{2+} was investigated by varying the concentration from 0 to 10 μM.

The selectivity of the fluorescent sensor

To evaluate the selectivity of the proposed fluorescent sensor, the following procedure was carried out. An individual stock solution of each of the various metal ions (0.01 mM), including Li^{+}, Na^{+}, K^{+}, Ba^{2+}, Ca^{2+}, Cd^{2+}, Co^{2+}, Cu^{2+}, Fe^{2+}, Fe^{3+}, Mg^{2+}, Mn^{2+}, Ni^{2+}, Pb^{2+}, Zn^{2+}, Cr^{3+} and Al^{3+} ions, was prepared by the dissolution of their metal salts in DI water. Then 100 μL of their stock solutions were added to 10 mL volumetric flasks each containing 1 mL of the GQDs (200 mg L^{-1}), 4 μM Hg^{2+}, and 70 μM TAA in a 0.1 M phosphate buffer solution with a pH of 7. Finally, the volume of the reaction mixture was adjusted to 10 mL with DI water.

Results and discussion

The characterization of the synthesized GQDs

Fig. 1(a) shows the UV-Vis absorption spectrum of the synthesized GQDs, which exhibits two absorption bands at around 230 nm. The broadened absorption band centered at 230 nm, resulting in nearly no fluorescence signal, is attributed to the π–π* electronic transition of the aromatic sp^2 domains.[22] The other typical absorption peak centered at 365 nm is assigned to the n–π* transition of the graphitic sp^2 domains.[23] The photoluminescence (PL) spectra of the synthesized GQDs show strong peaks at 460 nm when excited at 370 nm and the full width at

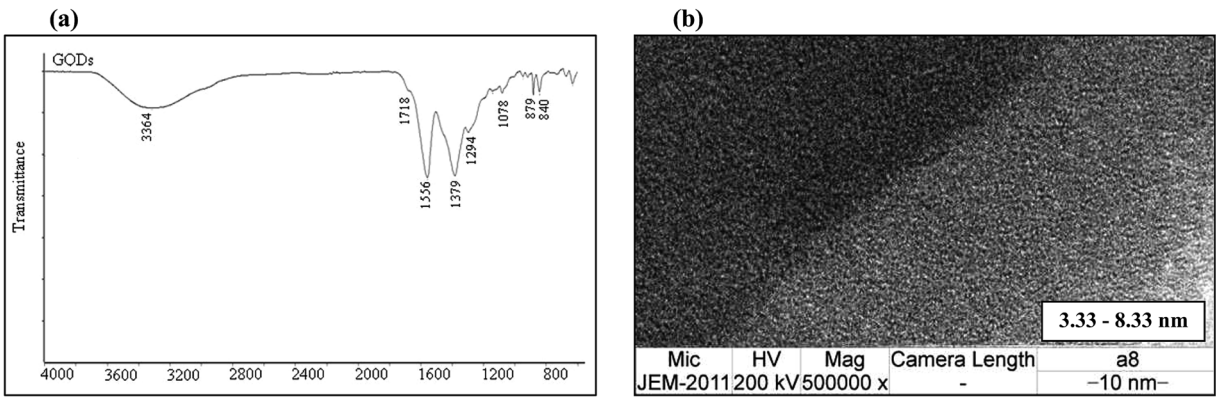

Fig. 2 (a) The FT-IR spectrum and (b) TEM image of the GQDs.

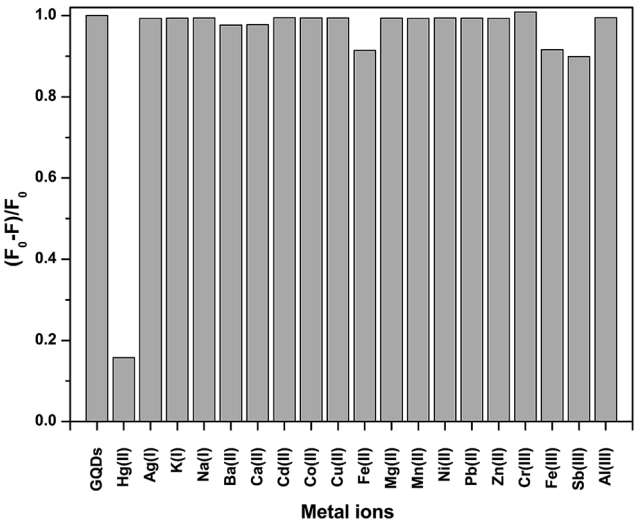

Fig. 3 The quenching of the fluorescence intensity of the GQDs by different metal ions. All the cation concentrations were 100 μM. *F* and F_0 are the emission intensities of the GQDs at 460 nm in the presence and absence of the metal ions.

half maximum (FWHM) is about 100 nm, which is approximately the same as those of most reported GQDs.[24]

To further characterize the optical properties of the synthesized GQDs, a detailed PL investigation was carried out with different excitation wavelengths (Fig. 1(b)). When the excited wavelengths change from 320 to 370 nm, the PL intensities increase markedly, but the fluorescence emission peak remains unshifted. This excitation-independent PL behavior is also attributed to a similar trend to the behaviour of previously reported GQDs.[25]

Fig. 2(a) shows the FT-IR spectrum of the GQDs. The strong bands at around 1556 cm^{-1} are due to the C=C stretching mode of polycyclic aromatic hydrocarbons,[26] indicating that the GQDs retain their graphene structure. Moreover, the bands at around 1718 cm^{-1} correspond to the carboxyl groups, and the bands at around 3440 cm^{-1} are attributed to the stretching vibrations of the hydroxyl groups. The peaks at 1364–1068 cm^{-1} are attributed to the C–O bond in the COH/COC (epoxy) groups.[27]

To determine the particle size of the obtained GQDs, the sample was characterized by transmission electron microscopy (TEM). Fig. 2(b) shows the image of the GQDs. Using image J software, the GQD particles, which had a diameter in the range of 3.33 nm to 8.33 nm, are shown to be distributed uniformly. The small particle size of the GQDs provides evidence for the fluorescence intensity.

The quenching effect of the metal ions on the fluorescence intensity of the GQDs

To test the effect of the metal ions on the fluorescence intensity of the GQDs, various cations were studied including Ag^{+}, K^{+}, Na^{+}, Ba^{2+}, Ca^{2+}, Cd^{2+}, Co^{2+}, Cu^{2+}, Fe^{2+}, Fe^{3+}, Hg^{2+}, Mg^{2+}, Mn^{2+}, Ni^{2+}, Pb^{2+}, Zn^{2+}, Cr^{3+}, Fe^{3+}, Sb^{3+}, and Al^{3+} as shown in Fig. 3.

From Fig. 3, it was clearly found that Hg^{2+} could quench the fluorescence intensity of the GQDs very strongly, while both the Fe^{2+} and Fe^{3+} ions had a slight quenching effect. The other ions scarcely quenched the fluorescence intensity of the GQDs. The high selectivity may be attributed to the fact that the Hg^{2+} ions have a stronger affinity towards the carboxylic groups on the GQD surface than other reported metal ions.[28] The quenching mechanism presumably occurs *via* either electron or energy transfer from the GQDs to the Hg^{2+} ions.[29]

The optimum conditions for the quenching effect of the GQDs by mercury ions

The optimum concentration of Hg^{2+} was studied as shown in Fig. 4(a) and (b). When the Hg^{2+} concentration increased, the emission intensity of the GQDs gradually decreased. A linear

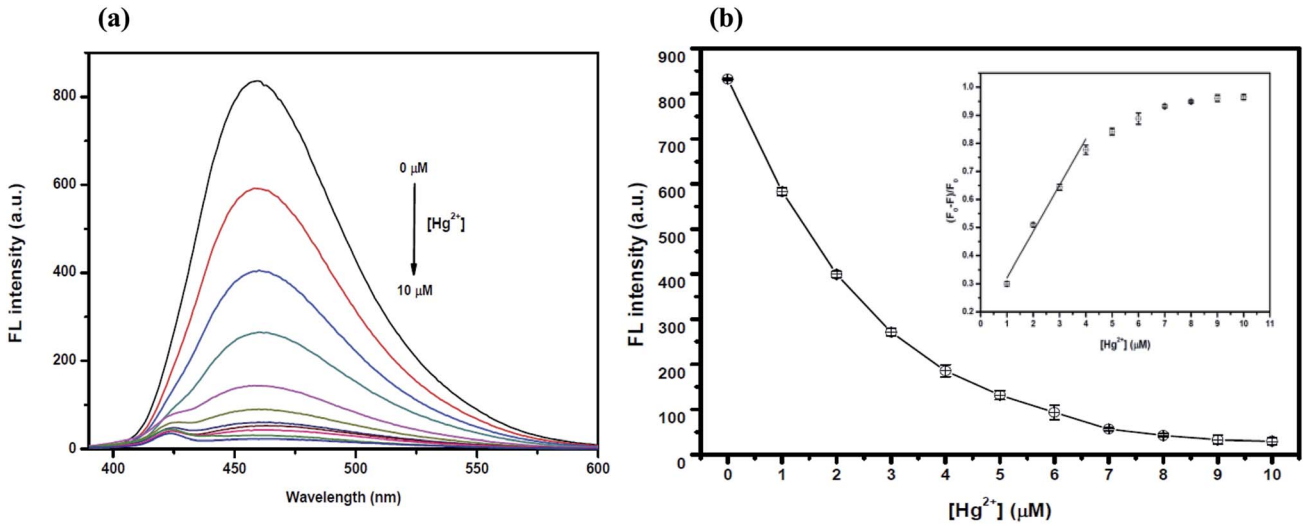

Fig. 4 (a) The changes in the emission spectra of the GQDs at different Hg^{2+} concentrations (0–10 μM) and (b) changes in the emission intensity at 460 nm *versus* the Hg^{2+} concentration (inset, the plot of $(F_0 - F)/F_0$ *versus* the concentration of Hg^{2+}).

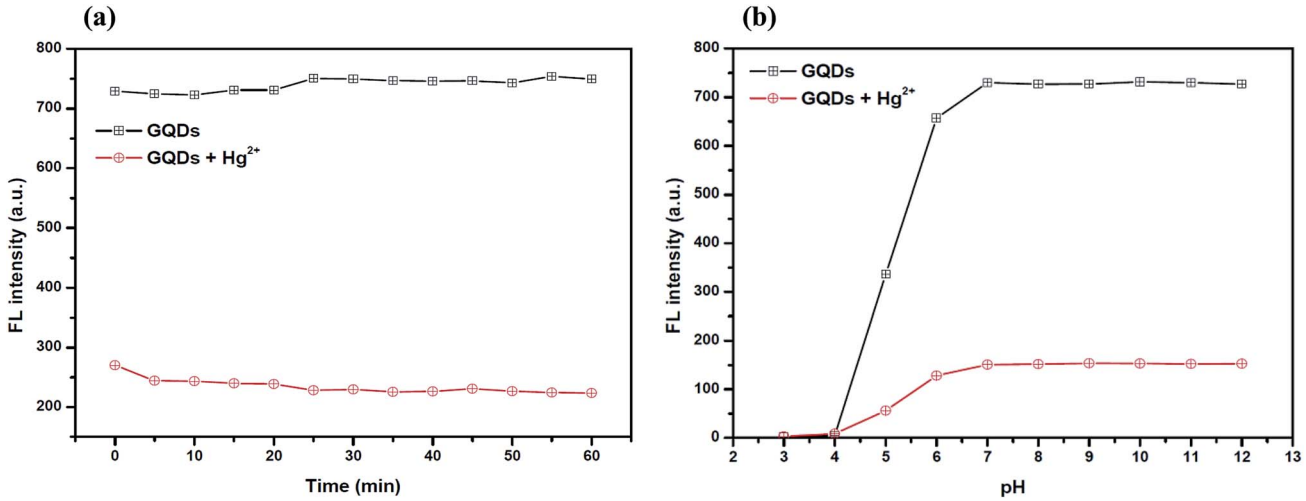

Fig. 5 (a) The changes in the fluorescence intensity of the GQDs at different reaction times. Conditions: 4 μM Hg^{2+} in 0.1 M phosphate buffer at a pH of 7.0 and (b) the changes in the fluorescence intensity of the GQDs at different values of pH. Conditions: 4 μM Hg^{2+} and 5 min reaction time.

relationship was obtained when the maximum intensity of the GQDs at 460 nm was plotted against the Hg^{2+} concentration in the range of 1–4 μM. When the concentration of Hg^{2+} was 4 μM, the fluorescence intensity of the GQDs was efficiently quenched. Therefore, 4 μM Hg^{2+} was used for the further studies.

To improve the quenching effect of Hg^{2+}, several experimental parameters were optimized including the reaction time and solution pH value. After the addition of 4 μM Hg^{2+}, the fluorescence (FL) spectrum of the GQDs (pH 7.0 and 20 mg L^{-1} GQDs), was recorded at every 5 min interval. Thus, the FL intensity of the GQDs at 460 nm decreased as much as 82% within a minute after the addition of Hg^{2+} (Fig. 5(a)), then the FL intensity gradually decreased until 5 min, and then finally it remained constant over the next 60 min. From the results, it is suggested that the quenching process is almost completed within 5 min.

For the effect of the pH, a series of acetate and phosphate buffers at different pH values were prepared, and then the GQD solutions (20 mg L^{-1} final concentration) together with 4 μM Hg^{2+} were added into each different buffer solution (pH: 3.0, 4.0, 5.0, 6.0, 7.0, 8.0, 9.0, 10.0, 11.0 and 12.0 in 0.1 M). The FL intensity was measured at 460 nm from each of the two buffered solutions of GQD only and GQDs with Hg^{2+} (Fig. 5(b)). The FL intensity of the GQDs increased gradually with pH values from 3.0–7.0 and stabilized under alkaline conditions. It was implied that a suitable quenching effect occurred with pH > 7.0. Thus, the working pH for a sufficiently sensitive and stable quenching of Hg^{2+} was 7.0.

The optimum conditions for the fluorescence turn-on of the Hg^{2+} quenched GQDs using the hydrolysis of thioacetamide

TAA is an active organosulfur, which undergoes hydrolysis giving hydrogen sulfide in the solution. As shown in reaction (1), the homogeneously generated hydrogen sulfide and sulfide ions (HS^- and S^{2-}) can act in similar roles to the thiol group, then they can bind to Hg^{2+} through Hg–S interactions. This causes the Hg^{2+}–GQD complex to dissociate, resulting in the restoration of the fluorescence intensity of the GQDs.[30]

$$CH_3CSNH_2 + 2H_2O \rightarrow CH_3CO_2^- + NH_4^+ + H_2S \quad (1)$$

To make sure that H_2S can have a fluorescence enhancing effect on the Hg^{2+}–GQDs, a common sulfide salt was used. In this regard, a solution of Na_2S was added to the Hg^{2+}–GQDs reaction mixture and then the fluorescence intensity of the GQD system was measured compared with that of the Hg^{2+}–GQDs mixture using TAA. From the results (Fig. 6), it was found that both kinds of the two sulfide solutions provided a similar trend, suggesting that the H_2S generated from TAA could enhance the fluorescence intensity of the Hg^{2+}–GQDs.

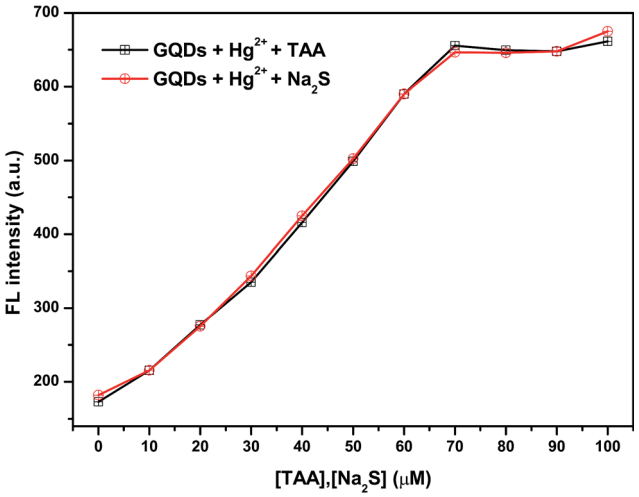

Fig. 6 The effect of different concentrations of TAA or Na_2S on the fluorescence intensity of the Hg^{2+}–GQDs.

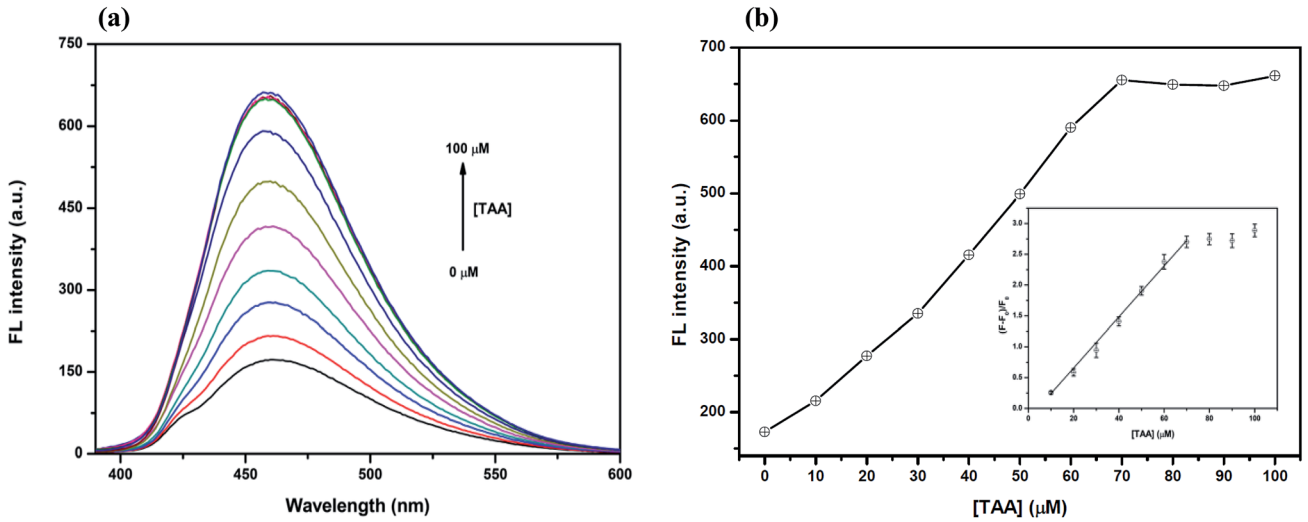

Fig. 7 (a) The changes in the FL spectra of the Hg^{2+}–GQDs at different TAA concentrations (0–100 μM). Conditions: 4 μM Hg^{2+} in a 0.1 M phosphate buffer with a pH of 7.0 and (b) the changes in the FL intensity at 460 nm *versus* the TAA concentration. Conditions: 4 μM Hg^{2+} in 0.1 M phosphate buffer with a pH of 7.0 (inset, plot of $(F_0 - F)/F_0$ *versus* the concentration of TAA).

However, the optimum concentration of TAA was also studied as shown in Fig. 7(a) and (b). When the concentration of TAA increased, the FL intensity of the Hg^{2+}–GQDs was gradually restored. A linear relationship was obtained when plotting the maximum intensity of the Hg^{2+}–GQDs at 460 nm against the TAA concentration in the range of 0–70 μM (Fig. 7(b)). At 70 μM TAA, the fluorescence intensity of the Hg^{2+}–GQDs was efficiently restored. Therefore, 70 μM TAA was selected for further studies.

Also, to improve the fluorescence restoration efficiency of the Hg^{2+}–GQD complex, the reaction time and pH value were optimized (Fig. 8(a)). After the addition of 70 μM TAA, the FL intensity of the GQD system (pH 7.0) was recorded every 5 min and it increased rapidly. The results suggested that the restoration process is completed within a minute.

To study the effect of the pH, 70 μM TAA was added to the Hg^{2+}–GQD complex in the buffer solution at different pH values. As the results show in Fig. 8(b), the FL intensity of the GQDs increased gradually with the pH increasing from 3.0–7.0 and stabilized under alkaline conditions. It is implied that a suitable FL enhancing effect occurred with pH > 7.0. Thus, the working pH of the hydrolysis of TAA for a sufficiently sensitive and stable FL enhancing effect was 7.0.

The optimum conditions for the fluorescence turn-off sensor for silver ions

The overall assay strategy for the sensing of Ag^{+} is shown in Fig. 9. The GQDs showed strong blue fluorescence in an

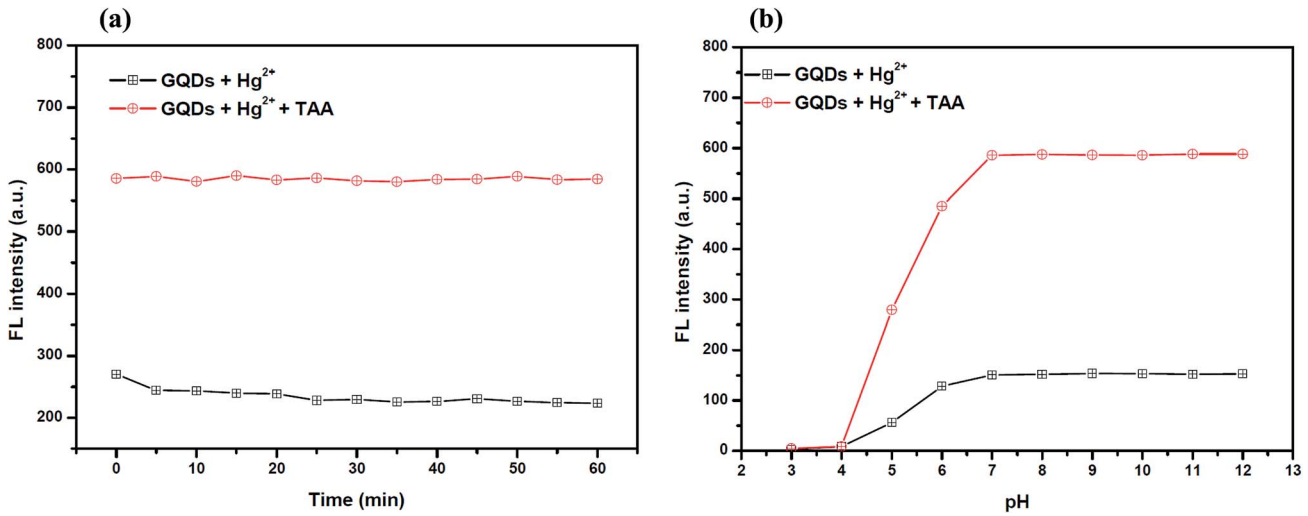

Fig. 8 (a) The changes in the FL intensity of the Hg^{2+}–GQDs at different reaction times. Conditions: 0.1 M phosphate buffer pH 7.0, 4 μM Hg^{2+} and 70 μM TAA and (b) the changes in the FL intensity of the Hg^{2+}–GQDs at different pH values. Conditions: 4 μM Hg^{2+}, 70 μM TAA and 5 min reaction time.

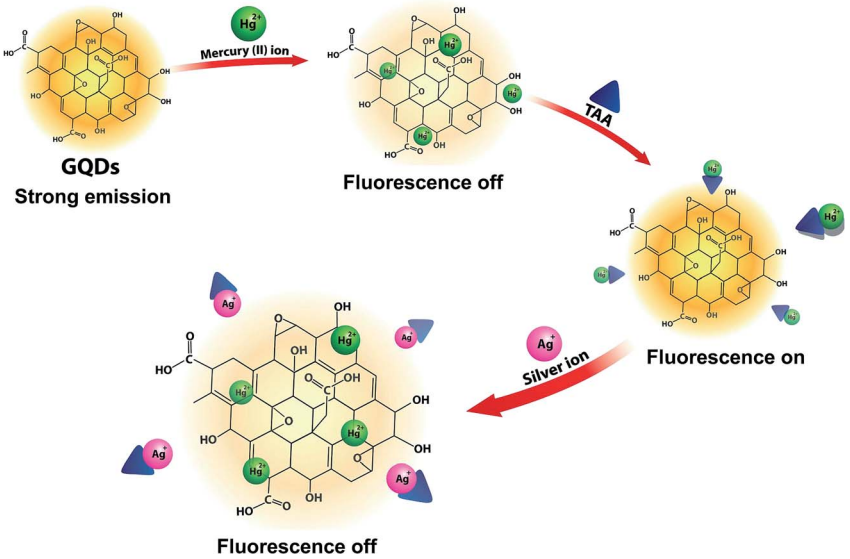

Fig. 9 A schematic illustration of the FL turn-off/on/off mechanism of the GQD-based Ag^+ sensing.

aqueous buffer solution. Upon the addition of Hg^{2+}, it bound to the GQDs resulting in fluorescence quenching of the GQDs. But when TAA was added, the TAA could react with the Hg^{2+} ion through Hg–S interaction. When the Hg^{2+}–GQD complex dissociated, the fluorescence of the GQDs was restored. Lastly, when Ag^+ ions were added to the reaction mixture, the fluorescence intensity of the GQDs decreased. The FL turn-off mechanism possibly occurs, and this means that the Ag^+ ion has more affinity to bind with a sulfur atom on the thiol group compared with the mercury ion. Thus, when Ag^+ was added to the mixture, it would bind with the sulfur atom of H_2S and break the Hg–S bond. Therefore, the free Hg^{2+} ion would bind to the GQDs again, leading to the fluorescence turn-off sensing of the GQD system.

As shown in Fig. 10(a), the fluorescence intensity of the GQDs gradually decreased when the concentration of Ag^+ increased. A linear relationship was obtained when the maximum intensity of the GQDs at 460 nm was plotted against the Ag^+ concentration in the range of 0.5–10 μM (Fig. 10(b)) with the Stern–Volmer plot shown in Fig. 10(c).

To improve the performance of the quenching of Ag^+, several experimental conditions, *i.e.* the reaction time and solution pH value, were optimized. After the addition of 10 μM Ag^+, the FL spectrum of the GQDs was recorded at five min intervals. The FL intensity of the quenched GQDs at 460 nm rapidly decreased and remained constant within 5 min (Fig. 11(a)), and the FL intensity remained constant over the next 60 min. The results suggest that the quenching process is completed within 5 min.

The effect of the pH on the FL sensing system was studied from pH 3–12 in two selected buffer solutions. 10 μM Ag^+ solution was added to the GQD solution at different pH values, as shown in Fig. 11(b). The FL intensity of the GQDs increased gradually from pH 3.0–7.0 and stabilized under the alkaline conditions. It is implied that the most suitable quenching effect occurred with pH > 7.0. Thus, the working solution pH for the Ag^+ quenching effect was also found to be 7.0.

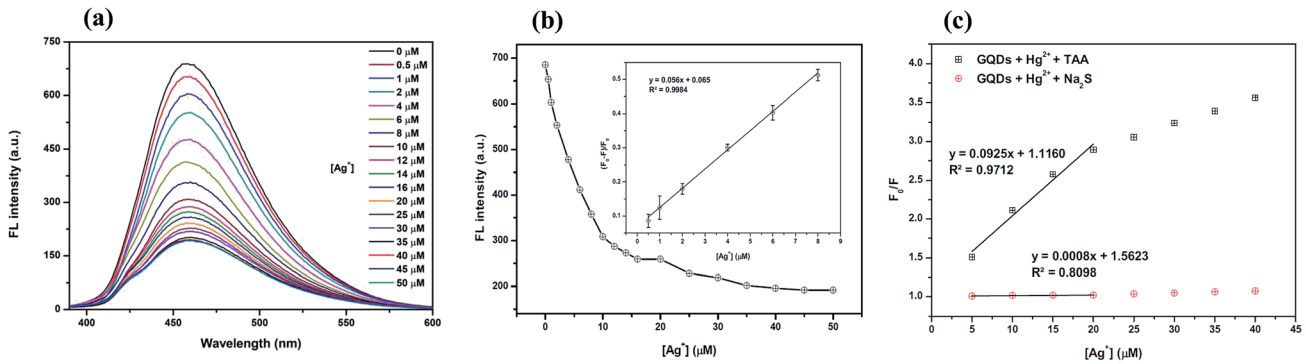

Fig. 10 (a) The changes in the FL intensity of the Hg^{2+}–GQDs at different Ag^+ concentrations (0–50 μM), (b) the changes in the FL intensity at 460 nm *versus* the Ag^+ concentration (inset, the plot of $(F_0 - F)/F_0$ *versus* the concentration of Ag^+) and (c) the Stern–Volmer plots of the Ag^+ quenching effect for both Hg^{2+}–GQDs in the presence of either TAA or Na_2S solution.

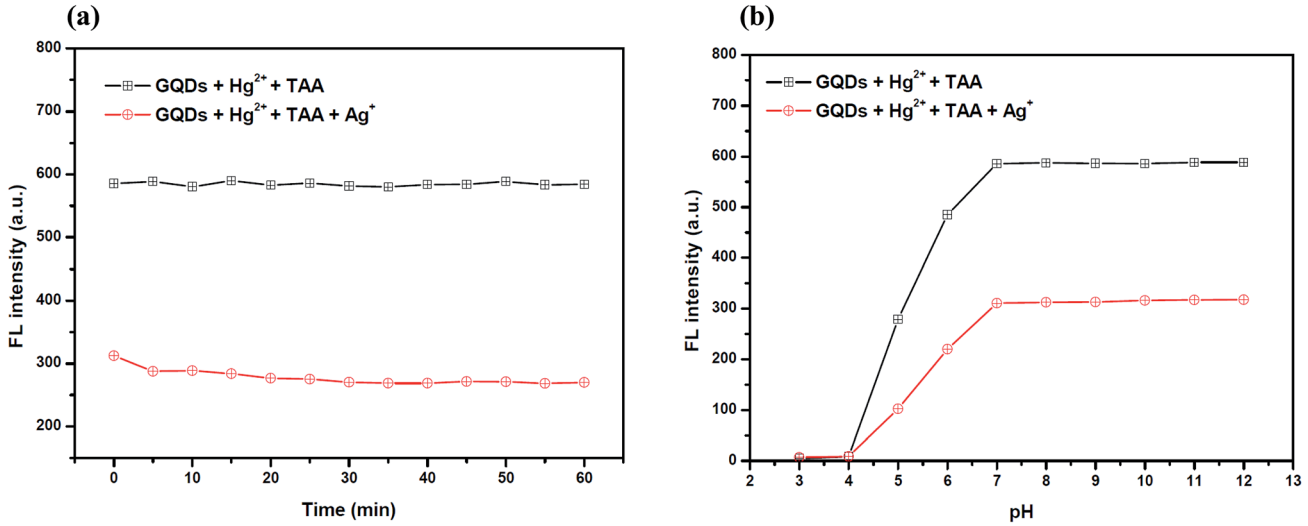

Fig. 11 (a) The changes in the FL intensity of the Hg^{2+}–GQDs at different reaction times. Conditions: 0.1 M phosphate buffer with a pH of 7.0, 4 μM Hg^{2+}, 70 μM TAA and 10 μM Ag^{+} and (b) the changes in the FL intensity of the Hg^{2+}–GQDs at different pH values. Conditions: 4 μM Hg^{2+}, 70 μM TAA, 10 μM Ag^{+} and a 5 min reaction time.

The selective determination of the silver ion

To study the selectivity of the developed GQD fluorescent sensor for Ag^{+} detection, the values of $(F - F_0)/F_0$ for the GQD system in the presence of 18 different cations, Ag^{+}, Li^{+}, Na^{+}, K^{+}, Ba^{2+}, Ca^{2+}, Cd^{2+}, Co^{2+}, Cu^{2+}, Fe^{2+}, Fe^{3+}, Mg^{2+}, Mn^{2+}, Ni^{2+}, Pb^{2+}, Zn^{2+}, Cr^{3+}, and Al^{3+}, were plotted using a 10 μM concentration of each metal. Fig. 12 shows that the addition of Ag^{+} to the reaction mixture of the GQD system resulted in fluorescence quenching, whereas the other remaining cations had no significant effects under the same experimental conditions.

Method validation

The analytical characteristics of the developed method were validated under the optimized conditions in terms of the linearity, limit of detection (LOD), limit of quantification (LOQ), precision and reproducibility (expressed as the relative standard deviation (RSD) of the calibration curve slope obtained from both intra-day and inter-day analysis) to estimate the efficiency and feasibility of the method for use with tap and drinking water samples. The linearity values are from 0.5–10.0 μM (R^2 = 0.9918). The linear calibration graph is as follows: $y = 32.14x + 63.66$ (where y is the fluorescence intensity and x is the concentration of Ag^{+}). The LOD, defined as 3SD/m (where SD is the standard deviation of the low concentration of Ag^{+} and m is the slope of the calibration graph), was 0.18 μM. While the LOQ, defined as 10SD/m, was 0.60 μM. The precision, which was

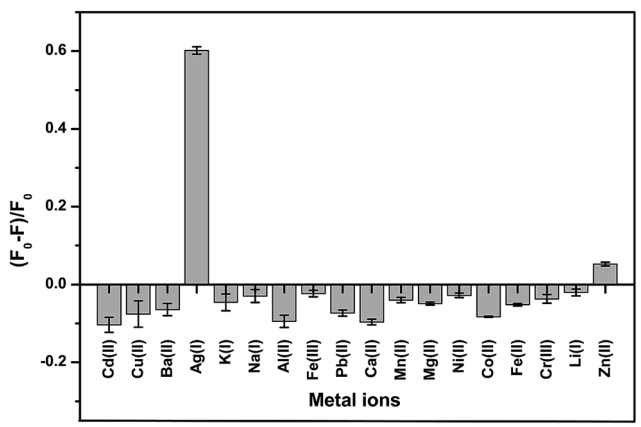

Fig. 12 The selectivity of the GQD FL sensor for different cations (10 μM) under the optimum conditions.

Table 1 The Ag^{+} content and recoveries of the water samples using the GQD system (n = 3)[a]

Sample	Added (μM)	Found (μM)	% recovery ± SD (μM)
Tap water	—	n.d.	—
	2	2.03	101.52 ± 2.99
	4	4.56	114.08 ± 2.99
	6	6.53	108.98 ± 3.49
Drinking water (Brand 1)	—	n.d.	—
	2	1.85	92.85 ± 4.17
	4	4.03	100.87 ± 1.08
	6	5.90	94.34 ± 3.18
Drinking water (Brand 2)	—	n.d.	—
	2	2.01	100.30 ± 4.15
	4	3.98	99.43 ± 4.34
	6	5.75	95.81 ± 1.02
Drinking water (Brand 3)	—	n.d.	—
	2	1.99	99.49 ± 3.13
	4	3.76	93.92 ± 1.74
	6	5.36	89.31 ± 2.61
Natural drinking water (Brand 4)	—	n.d.	—
	2	2.08	104.20 ± 4.76
	4	4.11	102.89 ± 2.56
	6	5.77	96.11 ± 1.97

[a] n.d. = not detected.

Table 2 The fluorescence turn-on/off sensor for Ag^+ detection using carbon based probes

Detection probe	Fluorescence mechanism	Linear range (μM)	Detection limit (μM)	Ref.
N-Doped C-dots	Enhancement	1–100	1.0	33
C-Dots	Enhancement	0–90	0.32	34
C-Dots	Enhancement	0.5–25	—	35
GQDs	Quenching	—	300	36
GQDs	Quenching	0.5–10	0.18	This work

evaluated in terms of the repeatability (data from 3 × 3 independent standard preparations, intra-day RSD), was 0.63% and the reproducibility (work performed during 11 × 3 consecutive days, inter-day RSD) was 2.45%, indicating an acceptable repeatability of the method.

The analysis of real samples

To demonstrate the applicability and reliability of the developed method, it was successfully applied to five water samples including tap water, three brands of drinking water (Brand 1, Brand 2, and Brand 3), and one brand of natural drinking water (Brand 4). The amounts of Ag^+ in each sample tested were obtained as shown in Table 1. The results showed that Ag^+ was not detected in all of these samples. In addition, to evaluate the matrix effect, the accuracy of the method was verified by calculating the recovery study in the real samples. Each sample was spiked with three concentrations (2.0, 4.0, and 6.0 μM) of the standard solution of Ag^+. Then, the relative percentage recoveries were calculated as follows:[31,32]

$$\% \text{ recovery} = [(C_{found} - C_{real})/C_{added}] \times 100 \quad (2)$$

where, C_{found}, C_{real}, and C_{added} are the concentration of the analyte found after the addition of a known amount of the standard in the real sample, the concentration of an analyte in the real sample, and the concentration of the known amount of standard that was spiked in the real sample, respectively. From the results (Table 1), it is evident that the recoveries of the developed method expressed as the mean percentage ($n = 3$) were in the range of 89.31–114.08%. This demonstrates that the method provides acceptable recovery for the determination of Ag^+ in these real samples, and its LOD is rather low as a trace level compared with other reported literature (Table 2). In addition, it can be concluded that the matrix has a negligible effect on the efficiency of the developed method.

Conclusion

A highly sensitive and selective fluorescent sensor for the detection of Ag^+ based on Hg^{2+} quenched GQDs in the presence of TAA was obtained. This novel approach based on GQDs for Ag^+ determination was carried out at a trace level. The GQDs were simply prepared from citric acid pyrolysis and characterized by molecular absorption and emission spectrophotometry, FT-IR spectroscopy and TEM. The optimum conditions for the fluorescence turn-on/off sensing probe, including the effects of the solution pH, the concentration of the GQDs, Hg^{2+}, Ag^+, and TAA, and the reaction time, were investigated. The Stern–Volmer plot for the Ag^+ quencher in the presence of homogeneously generated sulfide from TAA showed higher sensitivity compared with that of the common sulfide salt used.The selectivity of the fluorescence quenching for Ag^+ compared to various interfering metal ions was demonstrated. The analytical features of merit, including accuracy, precision, linearity, and limits of detection (LOD) and quantification (LOQ), were validated. The application of the developed method for the trace determination of Ag^+ in tap water and drinking samples was demonstrated.

Conflicts of interest

The authors have declared no conflict of interest.

Acknowledgements

The authors thank the Higher Education Research Promotion and National Research University Project of Thailand, the Office of the Higher Education Commission, the Food and Functional Food Research Cluster of Khon Kaen University, the Materials Chemistry Research Center, Department of Chemistry, and the Center of Excellence for Innovation in Chemistry (PERCH-CIC), Thailand for the financial support.

References

1 R. sedghi, M. Shojaee, M. Behbahani and M. R. Nabid, *RSC Adv.*, 2015, **5**, 67418–67426.
2 G. Absalan, M. Akhond, L. Sheikhian and D. M. Goltz, *Anal. Methods*, 2011, **3**, 2354–2359.
3 C. Z. Lai, M. A. Fierke, R. C. Costa, J. A. Gladysz, A. Stein and P. Buhlmann, *Anal. Chem.*, 2010, **82**, 7634–7640.
4 R. E. Godoy and A. G. Perez, *Analyst*, 1986, **111**, 1297–1299.
5 J. A. Lopez-Lopez, J. A. Jonsson, M. Garcia-Vargas and C. Moreno, *Anal. Methods*, 2014, **6**, 1462–1467.
6 E. Kariptas, C. Er, E. Kiray and H. Ciftci, *Anal. Methods*, 2016, **8**, 4285–4292.
7 L. M. Hallerstig, P. Granath, L. Lindgren and M. Tranberg, *Anal. Methods*, 2017, **9**, 149–153.
8 L. Liu, C. Wang and G. Wang, *Anal. Methods*, 2013, **5**, 5812–5822.
9 S. Zhan, Y. Wu, L. He, F. Wang, X. Zhan, P. Zhou and S. Qiu, *Anal. Methods*, 2012, **4**, 3997–4002.
10 D.-S. Lin, J.-P. Lai, H. Sun, Z. Yang and Y. Zuo, *Anal. Methods*, 2014, **6**, 1517–1522.
11 M. M. Rahman and A. M. Asiri, *RSC Adv.*, 2015, **5**, 63252–63263.
12 P. Sricharoen, N. Limchoowong, Y. Areerob, P. Nuengmatcha, S. Techawongstien and S. Chanthai, *Ultrason. Sonochem.*, 2017, **37**, 83–93.
13 N. Limchoowong, P. Sricharoen, Y. Areerob, P. Nuengmatcha, T. Sripakdee, S. Techawongstien and S. Chanthai, *Food Chem.*, 2017, **230**, 388–397.

14 Y. Dong, J. Shao, C. Chen, H. Li, R. Wang, Y. Chi, X. Lin and G. Chen, *Carbon*, 2012, **50**, 4738–4743.
15 S. Zhu, S. Tang, J. Zhang and B. Yang, *Chem. Commun.*, 2012, **48**, 4527–4539.
16 Z. Fan, S. Li, F. Yuan and L. Fan, *RSC Adv.*, 2015, **5**, 19773–19789.
17 S. Zhou, H. Xu, W. Gan and Q. Yuan, *RSC Adv.*, 2016, **6**, 110775–110788.
18 L. Liu, D. Zhang, G. Zhang, J. Xiang and D. Zhu, *Org. Lett.*, 2008, **10**, 2271–2274.
19 X. Zhu, S. Fu, W. K. Wong and W. Y. Wong, *Tetrahedron Lett.*, 2008, **49**, 1843–1846.
20 L. Liu, G. X. Zhang, J. F. Xiang, D. Q. Zhang and D. B. Zhu, *Org. Lett.*, 2010, **10**, 4581–4584.
21 F. Wang, R. Nandhakumar, J. H. Moon, K. M. Kim and J. Y. Lee, *Inorg. Chem.*, 2011, **50**, 2240–2245.
22 K. S. Novoselov, A. K. Geim, S. V. Morozov, D. Jiang, Y. Zhang and S. V. Dubono, *Science*, 2004, **306**, 666–669.
23 M. Xie, Y. Su, X. Lu, Y. Zhang, Z. Yang and Y. Zhang, *Mater. Lett.*, 2013, **93**, 161–164.
24 Y. Li, Y. Hu, Y. Zhao, G. Shi, L. Deng and Y. Hou, *Adv. Mater.*, 2011, **23**, 776–780.
25 S. K. Cushing, L. Ming, F. Huang and N. Wu, *ACS Nano*, 2014, **8**, 1002–1013.
26 X. Wang, X. Sun, J. Lao, H. He, T. Cheng, M. Wang, S. Wang and F. Huang, *Colloids Surf., B*, 2014, **122**, 638–644.
27 H. Wang, Q. Hao, X. Yang, L. Lu and X. Wang, *Electrochem. Commun.*, 2009, **11**, 1158–1161.
28 F. Chai, T. Wang, L. Li, H. Liu, L. Zhang, Z. Su and C. Wang, *Nanoscale Res. Lett.*, 2010, **5**, 1856–1860.
29 W. B. Lu, X. Y. Qin, S. Liu, G. H. Chang, Y. W. Zhang, Y. L. Luo, A. M. Asiri, A. O. Al-Youbi and X. P. Sun, *Anal. Chem.*, 2012, **84**, 5351–5357.
30 Z. Wu, W. Li, J. Chen and C. Yu, *Talanta*, 2014, **119**, 538–543.
31 P. Sricharoen, N. Limchoowong, T. Sripakdee, P. Nuengmatcha and S. Chanthai, *Anal. Methods*, 2017, **9**, 3810–3818.
32 P. Sricharoen, N. Limchoowong, S. Techawongstien and S. Chanthai, *Food Chem.*, 2016, **203**, 386–393.
33 Z. S. Qian, J. J. Ma, X. Y. Shan, H. Feng, L. X. Shao and J. R. Chen, *Chem.–Eur. J.*, 2014, **20**, 2254–2263.
34 X. Gao, Y. Lu, R. Zhang, S. He, J. Ju, M. Liu, L. Lia and W. Chen, *J. Mater. Chem. C*, 2015, **3**, 2302–2309.
35 X. L. Li, Y. W. He, J. S. Ryu and S. I. Yang, *New J. Chem.*, 2014, **38**, 503–506.
36 A. Suryawanshi, M. Biswal, D. Mhamane, R. Gokhale, S. Patil, D. Guin and S. Ogale, *Nanoscale*, 2014, **6**, 11664–11670.